Since January 2020 Elsevier has created a COVID-19 resource centre with free information in English and Mandarin on the novel coronavirus COVID-19. The COVID-19 resource centre is hosted on Elsevier Connect, the company's public news and information website.

Journal of Drug Delivery Science and Technology 75 (2022) 103625

Contents lists available at ScienceDirect

Journal of Drug Delivery Science and Technology

journal homepage: www.elsevier.com/locate/jddst

Opinion paper

Remdesivir-loaded bis-MPA hyperbranched dendritic nanocarriers for pulmonary delivery

Eleftherios Halevas [a,*], Barbara Mavroidi [a], Chrysoula Kokotidou [b,c], Alexandra Moschona [e,f], Marina Sagnou [a], Anna Mitraki [b,c], George Litsardakis [d], Maria Pelecanou [a]

[a] Institute of Biosciences & Applications, National Centre for Scientific Research "Demokritos", 15310, Athens, Greece
[b] Department of Materials Science and Technology University of Crete, Heraklion, 70013, Crete, Greece
[c] Institute for Electronic Structure and Laser FORTH N. Plastira 100, Heraklion, 70013, Crete, Greece
[d] Laboratory of Materials for Electrotechnics, Department of Electrical and Computer Engineering, Aristotle University of Thessaloniki, Thessaloniki, 54124, Greece
[e] Laboratory of Organic Chemistry, Department of Chemical Engineering, Aristotle University of Thessaloniki, Thessaloniki, 54124, Greece
[f] Laboratory of Natural Resources and Renewable Energies, Chemical Process and Energy Resources Institute, Centre for Research and Technology-Hellas (CERTH), Thessaloniki, 57001, Greece

ARTICLE INFO

Keywords:
Remdesivir encapsulation and delivery
2,2-bis(hydroxymethyl)propionic acid
hyperbranched dendritic nanocarriers
Bioavailable remdesivir nanocarriers
Nontoxic remdesivir nano-formulations

ABSTRACT

Remdesivir is the only clinically available antiviral drug for the treatment of COVID-19. However, its very limited aqueous solubility confines its therapeutic activity and the development of novel inhaled nano-based drug delivery systems of remdesivir for enhanced lung tissue targeting and efficacy is internationally pursued. In this work 2,2-bis(hydroxymethyl)propionic acid (bis-MPA) hyperbranched dendritic nano-scaffolds were employed as nanocarriers of remdesivir. The produced nano-formulations, empty and loaded, consisted of monodisperse nanoparticles with spherical morphology and neutral surface charge and sizes ranging between 80 and 230 nm. The entrapment efficiency and loading capacity of the loaded samples were 82.0% and 14.1%, respectively, whereas the release of the encapsulated drug was complete after 48 h. The toxicity assays in healthy MRC-5 lung diploid fibroblasts and NR8383 alveolar macrophages indicated their suitability as potential remdesivir carriers in the respiratory system. The novel nano-formulations are non-toxic in both tested cell lines, with IC_{50} values higher than 400 μM after 72 h treatment. Moreover, both free and encapsulated remdesivir exhibited very similar IC_{50} values, at the range of 80–90 μM, while its aqueous solubility was increased, overall presenting a suitable profile for application in inhaled delivery of therapeutics.

1. Introduction

Remdesivir, sold under the brand name Veklury®, is a broad-spectrum antiviral medication developed by Gilead Sciences [1]. It was proposed in 2009 as a potential treatment against hepatitis C and with limited effects against the Ebola outbreak in Congo in 2017. Remdesivir was also found to be effective against a broad range of animal and human coronaviruses (CoV) such as the Severe Acute Respiratory Syndrome (SARS-CoV-1) and the Middle East Respiratory Syndrome (MERS-CoV) coronaviruses. When the highly transmissible SARS-CoV-2 emerged in late 2019 in China, resulting in the global COVID-19 pandemic, remdesivir was one of the most effective clinical candidates that drew attention as a putative therapeutic weapon against the disease [2]. In fact, remdesivir is the only clinically available antiviral drug that has been approved by the US and European authorities for the treatment of COVID-19 in hospitalized adult and pediatric patients [3].

Remdesivir is the phosphoramidate prodrug of an adenosine analog acting as inhibitor of viral RNA synthesis (Fig. S1, Supplementary Materials). The prodrug diffuses into cells where it is metabolized into the active nucleoside triphosphate derivative, which competes with its natural counterpart for incorporation by the viral RNA-dependent RNA polymerase [1]. In the marketed product Veklury®, remdesivir (100 mg) is administered by intravenous infusion and because of its very limited aqueous solubility, sulfobutylether β-cyclodextrin sodium is included in the formulation to increase solubility [4]. However, recent reports suggest that the current mode of administration is unlikely to produce sufficiently high concentrations of remdesivir and its active metabolites in the lungs to effectively eliminate SARS-CoV-2 [5]. This fact, in combination with the

* Corresponding author.
E-mail address: lefterishalevas@gmail.com (E. Halevas).

https://doi.org/10.1016/j.jddst.2022.103625
Received 9 December 2021; Received in revised form 6 July 2022; Accepted 20 July 2022
Available online 10 August 2022
1773-2247/

reported adverse reactions (ADRs) associated with systemic administration [6], are shifting attention on inhaled nano-formulations of remdesivir to enhance lung tissue targeting and efficacy [7].

Pulmonary drug delivery nanotechnology is a relatively new concept and has become an appealing route to treat lung diseases. Nano-based drug delivery systems such as micelles, liposomes and lipid-based carriers [8], chitosan-poly(lactic-co-glycolic) acid nano-formulations [9-11], or polymeric nanoparticles [12] are designed to enhance the effectiveness of drugs at targeted lung regions, as well as lower dose-related toxicities and ADRs in non-target organs [6-13]. Already, in the fight against COVID-19, actively investigated therapeutic strategies employ nanoparticles [14,15]. In recent publications, anti-inflammatorry dexamethazone - the first drug to show life-saving efficacy in patients infected with SARS-CoV-2 - is investigated as a liposomal formulation targeting pulmonary macrophages or other immune cells for more effective anti-oedema and anti-fibrotic effect [16]. Furthermore, nanospray inhalation of remdesivir and hydroxychloroquinone using poly(lactic-co-glycolic) acid nanocarriers [17], as well as aerosolized remdesivir nanoliposomal carriers [18], are proposed as effective alternatives for COVID-19 treatment. As the SARS-CoV-2 infects primarily through the respiratory tract (upper airways and lungs) and mainly affects the lungs, the use of inhaled delivery becomes increasingly important for the non-invasive, quick and direct administration of therapeutics [19]. The fact that Gilead has initiated clinical testing of an inhaled solution of remdesivir [20] serves to intensify the importance of inhaled delivery for treatment of COVID-19 and validate all efforts in the field.

Within this framework, in continuation of our investigations in nano-formulations for effective and safe delivery of hydrophobic cargo [21,22], and aspiring to contribute to the above reported efforts [16–18] for an inhaled formulation of remdesivir, we present herein the employment of the dendritic-linear-dendritic (DLD) bis-MPA hyperbranched dendritic scaffold (HDS, and specifically, the bis-MPA PEG6k-OH, pseudo generation 4, Fig. S2, Supplementary Materials) in the synthesis of remdesivir-loaded nano-formulations. The employed HDS comprises two hyperbranched bis-MPA blocks attached through ester bonds to a middle hydrophilic PEG chain and belongs to a group of dendritic scaffolds suitable for biomedical applications [23–25]. The novel remdesivir-loaded nanomaterials (mentioned henceforth as RHDSs and their empty counterparts as EHDSs) were characterized by physico-chemical and electron microscopy techniques, and evaluated for their suitability as potential remdesivir carriers in the respiratory system through release studies and toxicity assays in healthy MRC-5 lung diploid fibroblasts and NR8383 alveolar macrophages.

2. Experimental

2.1. Materials and methods

All necessary information regarding materials and equipment used are provided in Supplementary Materials.

2.2. Synthesis of RHDSs

A modification of the oil-in-water (O/W) single emulsion/solvent evaporation method [26–28] was applied for the formulation of the remdesivir-loaded HDSs, according to our previously reported work [21]. Specific details are provided in Supplementary Materials.

2.3. Determination of remdesivir loading capacity and entrapment efficiency

The determination of the loading capacity and entrapment efficiency of remdesivir into the hyperbranched dendritic nanocarriers was performed via HPLC analysis. The procedure is described in detail in Supplementary Materials.

2.4. In vitro remdesivir release study

The release of remdesivir from RHDSs was monitored with HPLC. The procedure is described in detail in Supplementary Materials.

2.5. 5. Biological evaluation

The remdesivir concentration in all solutions employed in biological evaluation was estimated using the determined loading capacity of the RHDSs and the release curve (Fig. 3A), according to our previously reported work [21]. The MTT (3-[4,5-dimethylthiazol-2-yl]-2,5-diphenyl-tetrazolium bromide) assay was employed according to a published procedure [21,29]. Specific details are provided in Supplementary Materials.

Cell cultures (MRC-5 and NR8383 cells) were developed according to published protocols [30,31] with slight modifications. Specific details are provided in Supplementary Materials.

3. Results and discussion

3.1. Synthesis of RHDSs

The RHDSs were synthesized according to a firstly applied on bis-MPA hyperbranched dendritic systems modification of the oil-in-water (O/W) single emulsion/solvent evaporation method [26–28], a process commonly applied for the encapsulation of hydrophobic molecules, as remdesivir. The synthesis was carried out through the addition of the organic phase with dissolved remdesivir to the aqueous (Phosphate buffered saline, PBS) DLD-polymer solution, followed by high-speed homogenization of the generated emulsion, sonication, and

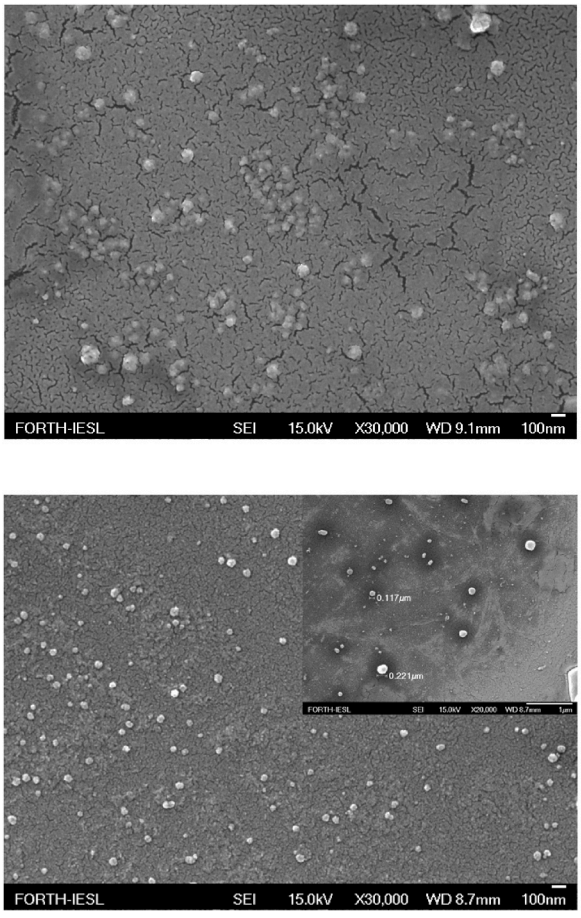

Fig. 1. A) FESEM images of EHDSs (at 100 nm) and B) FESEM images of RHDSs (at 100 nm, inset photo at 1 μM).

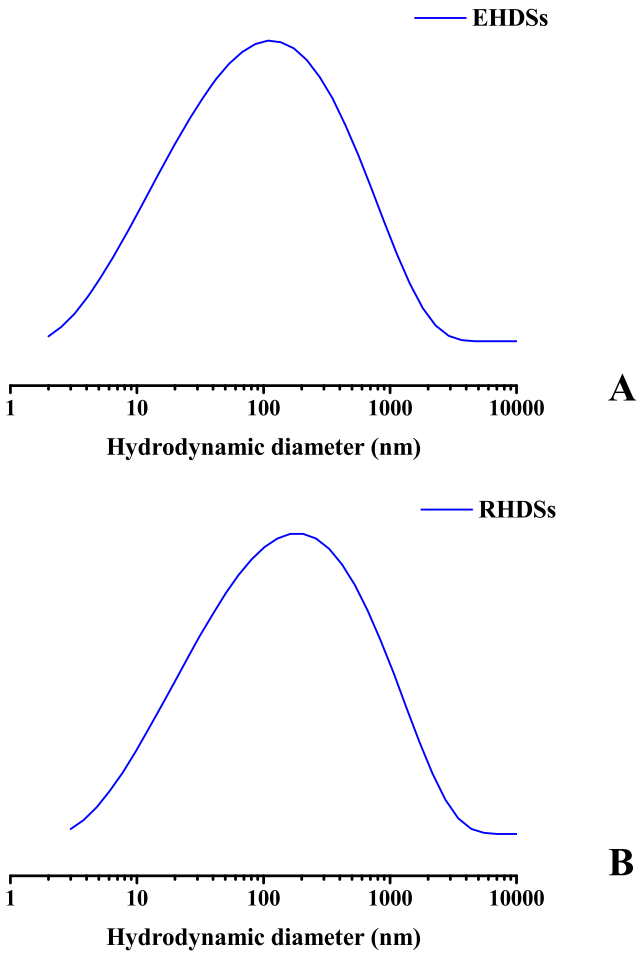

Fig. 2. Particle size distribution of A) EHDSs and B) RHDSs.

subsequent evaporation of the organic solvents, resulting in the precipitation of the remdesivir-loaded hyperbranched dendritic nano-scaffolds, which were collected with centrifugation. Addition of emulsifying agent in the preparation mixture was not necessary, as the DLD polymer is soluble in the employed organic and aqueous solvents and the long PEG chain in its structure acts as viscosity regulator [32]. The remdesivir molecules are encapsulated within the dendritic nano-carriers through weak van der Waals forces and hydrogen bonds with the functional groups of the HDSs [33,34]. It is worth noting that the molecule of remdesivir has 4 hydrogen bond donor atoms and 13 hydrogen bond acceptor atoms in its structure [35] that may well interact with the 32 hydroxyl groups of the polymer as well as with hydrogen bond acceptor oxygens of the PEG chain. The applied remdesivir-to-dendrimer molar ratio during synthesis was ≈1:1.5 to ensure sufficient excess of the carrier for the optimum entrapment of remdesivir and avoid drug precipitation. As the emerging nano-formulations are particularly hydrophilic, they were meticulously dried under vacuum before their further physico-chemical characterization and biological evaluation.

3.2. FT-IR spectroscopy

In the Fourier-transform infrared (FT-IR) spectrum of RHDSs (Fig. S3, Supplementary Materials) peaks associated with both remdesivir and the DLD-polymer are present. More specifically, the O–H stretching vibrations are detected as a broad band centered around 3398 cm^{-1}. The small shoulder located at around 2943 cm^{-1} is assigned to the asymmetrical stretching vibrations of the $–CH_3$ groups of the bis-MPA hyperbranched units whereas the strong absorption band located at 2883 cm^{-1} is typical of the C–H stretching vibrations of the bis-MPA units and the PEG chain [36,37]. The strong absorption band located at 1467 cm^{-1} is characteristic of the $–CH_3$ asymmetric bending vibrations (bis-MPA dendron) and the bending vibrations of $–CH_2$ (PEG chain, bis-MPA dendron). Moreover, the sharp absorption band located at 1732 cm^{-1} is attributed to the carboxylate C═O stretching vibrations (bis-MPA dendron). The C–O stretching vibrations are located around 1344 cm^{-1} and 1280 cm^{-1} as a medium and a weak band, respectively. Moreover, the strong bands at 963 cm^{-1} and 842 cm^{-1} are indicative of the C–C stretching vibrations [36,37]. The absorption bands at 1240 cm^{-1} and 1209 cm^{-1} can be assigned to the P═O absorption [38]. The sharp absorption bands at 1153 cm^{-1} and 1042 cm^{-1} are characteristic for the P–N and the P–O–C stretching vibrations [39,40], respectively.

3.3. FESEM analyses

Representative field emission scanning electron microscopy (FESEM) images of EHDSs and RHDSs (Fig. 1A and B) show that the EHDS sample consists of spherical, relatively monodisperse nanoparticles, with a relatively narrow size distribution between 80 and 120 nm. In the case of the RHDSs the presence of distinct globular nanoparticles with diameters between 100 and 230 nm and a wide particle size distribution is observed. The consequent increase in the diameter of the RHDSs in comparison to that of EHDS species is in accordance with the entrapment of remdesivir molecules within the dendritic nano-cavities and the consequent swelling of the nanocarrier. The size range of the generated nano-formulations is considered suitable for efficient cell uptake and low immunogenic response [41]. Most importantly, it is ideal for respiratory tract direct applications, as inhalation of powder particles with diameters below 5 μm can lead to the efficient delivery into the lower part of the respiratory tract [17].

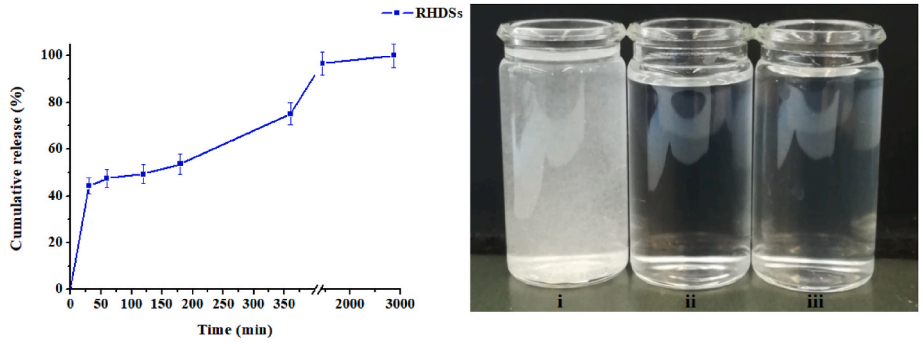

Fig. 3. A) Cumulative release percentage of remdesivir with regard to the total entrapped remdesivir vs. time and B) from left to right: i) remdesivir dispersed in PBS, ii) EHDSs dispersed in PBS, and iii) RHDSs dispersed in PBS after 48 h of release study.

3.4. Particle size analysis and z-potential

Z-potential and DLS measurements were carried out in order to further estimate the surface charge and the mean hydrodynamic diameter (Fig. 2A and B) of the EHDS and RHDS species. The mean hydrodynamic diameter of EHDSs and RHDSs was determined to be 109.0 ± 18.7 nm and 185.0 ± 30.5 nm, respectively. The results are in complete agreement with the FESEM observations and indicate the effect of remdesivir encapsulation on the size of the emerging nanocarriers. The z-potential value of EHDSs was estimated to be 1.0 ± 0.2 mV, verifying the neutral surface charge of bis-MPA HDSs, whereas the z–potential of RHDSs was −7.0 ± 0.6 mV. As expected, encapsulation of the neutral remdesivir molecules at pH 7.4 (PBS), had no effect on the surface charge of the generated nano-formulations. Although the observed z–potential values of both empty and remdesivir-loaded samples in solution were relatively low and could have affected the stability of the produced nano-formulations inducing the formation of large secondary aggregates due to weak repulsive forces, no significant aggregation was observed. It is likely that the employed hyperbranched G4-PEG6k-OH dendrimer could have provided an effective shielding potentially attributed to its low core-to-PEG ratio and hence a high PEG surface density, resulting thus in improved stealth properties or steric repulsion between the HDSs during remdesivir loading [25,27,42]. The observed slightly negative or neutral z-potential values of the generated nano-formulations are suited for bio-applications, as they are considered ideal for membrane penetration and tissue absorption [43,44].

3.5. Loading capacity and entrapment efficiency

The *in situ* loading capacity and entrapment efficiency of remdesivir in HDSs was estimated to be 82.0% and 14.1%, respectively. The obtained results can be considered sufficiently good and favorably compare to those reported for other types of remdesivir nanocarriers [18]. The production of hydrophilic nano-formulations with a heavily entrapped organic compound points out the potential of the relatively unexplored G4-PEG6k-OH HDSs as carriers of pharmacophores. The relatively high loading capacity and entrapment efficiency of remdesivir can be assigned to the large length of the PEG chain and the high generation of the employed DLD-polymer, as also observed in other literature reports [28,45–47]. In general, long PEG chains and dendritic polymers of high generation form bulkier dendritic cavities, thus resulting in larger inner space and less dense conformations that enhance the degree of encapsulation [28,45–47].

3.6. Release study

The release profile of the encapsulated remdesivir is a crucial parameter for the determination of the pharmacokinetic behavior of RHDSs. Fig. 3A shows the percentage of remdesivir released in PBS pH 7.4 with regard to the total entrapped remdesivir versus time. The results show complete release of remdesivir from the RHDSs during the 48-h study, indicating total dissolution of the nano-formulations. By examining the release profile, it can be seen that up to the first 30 min there is an initial burst release of ~45% of the initial remdesivir present, mainly attributed to loosely bound or adsorbed remdesivir molecules on the large surface of the nanoparticle [48,49]. This initial rapid release is followed by a slower release phase between 60 and 180 min, reaching a plateau after 24 h, probably associated with penetration of water into the nanoparticle, the dissolution of remdesivir and its diffusion into the aqueous medium. This continuous and sustained release indicates that remdesivir is well entrapped in the HDSs. The observed complete release of remdesivir may be related with the high hydrophilicity of the HDSs, the high PEG molecular weight (6 kDa) and the low aggregation rate of the produced nano-formulations [42]. Specifically, the presence of 32 hydroxyl groups on the hyperbranched G4-PEG6k-OH polymer, as well as the embedded hydrophilic PEG-chain in its structure, render the generated nano-formulations completely miscible with water and contribute to the efficient remdesivir release.

Furthermore, it should be noted that despite the lack of aqueous solubility of remdesivir (0.028 mg mL^{-1} at room temperature) [50], no precipitation of the drug is taking place, as also visually exhibited in Fig. 3B. Based on the release measurements in PBS pH 7.4 after 48 h, the dissolved remdesivir was calculated to be 0.24 mg mL^{-1}, while the resulting concentration of the dissolved bis-MPA nanocarriers in the PBS solution was 1.43 mg mL^{-1}. The obtained results indicate the enhanced aqueous solubility of remdesivir, induced by its formulation with the bis-MPA (G4-PEG6k-OH) dendritic scaffold, and favorably compare to other literature reported results on remdesivir nanocarriers [17,18] and formulations with Tween-80, PEG-400, or sulfobutylether-beta-cyclodextrin (SBECD) [48]. The release data of remdesivir from the RHDSs were fitted to several kinetic equations (zero order, first order, Higuchi, Korsmeyer-Peppas, Hixson-Crowell). The mathematical model which very satisfactorily describes the release kinetics is the first order model, with a high correlation coefficient $R^2 \approx 0.997$ (Fig. S4A, Supplementary Materials). First order kinetics are suggestive of concentration and time dependent release of the hydrophobic drug from the hydrophilic matrix [51–54]. Further fitting of the data to the Korsmeyer–Peppas equation ($R^2 \approx 0.937$, Fig. S4B, Supplementary Materials) led to the determination of the exponent of release n value of 0.267. According to the Korsmeyer–Peppas model, $n < 0.45$ points out that drug release is governed by diffusion according to the Fickian diffusion mechanism [49–55].

A summary of the physico-chemical characteristics of the produced empty and remdesivir-loaded nano-formulations is presented in Supplementary Material Table S1.

3.7. Stability studies

The stability of the produced RHDSs was evaluated via FESEM (Fig. S5, Supplementary Materials) and z-potential measurements after storage in PBS solution (pH 7.4) at 4 °C for two months. The nano-formulations did not show significant morphological alterations (eg. caking or phase separation) or extensive aggregation phenomena maintaining their surface charge above −10 ± 0.8 mV, thus indicating their stable profile over long time periods.

3.8. Biological activity

In order to assess the suitability of the generated nano-formulations for biological applications, the toxicity of the EHDSs and RHDSs against the healthy MRC-5 lung fibroblasts, a cell line that is commonly utilized in vaccine development as transfection host [29], and NR8383 alveolar macrophages that play a critical role in pulmonary defense and inflammatory responses [30], was determined with the MTT assay. Free remdesivir was also employed for comparison purposes. The results obtained after 72 h of exposure of the cells to EHDSs, RHDSs, and remdesivir are given in Table 1, while the IC_{50} curves are given in Fig. S6, Supplementary Materials. The first result to be noted is that EHDSs do not show any significant degree of cytotoxicity as their recorded IC_{50} values in both tested cell lines range over 400 μM at 72 h incubation time. The recorded complete lack of toxicity of the produced EHDSs nanomaterials in the tested cell lines is in complete agreement to our previous publication where it was shown that they were non-toxic towards breast cancer cells and healthy fibroblasts [20], and strongly advocates the biocompatibility of the bis-MPA dendritic scaffold. The second positive result to be noted is that RHDSs give IC_{50} values in the same concentration range as free remdesivir (80–90 μM in our study), in complete agreement to IC_{50} values reported in the literature in other cell lines, like MRC-5 [56] and Vero and Calu-3 [57], indicating that the presence of the bis-MPA dendritic scaffold does not alter the biological effect of released remdesivir on human cells, which remains at the usual levels of toxicity.

Table 1
Cytotoxicity of RHDSs, EHDSs, and free remdesivir, against MRC-5 and NR8383 cells evaluated by means of the MTT viability assay after 72 h of incubation. Values represent the mean ± standard deviation (SD) of IC_{50} values (μM) obtained in three independent experiments.

	IC_{50} (μM)	
	MRC-5	NR8383
EHDSs	447.71 ± 19.59	525.55 ± 14.99
RHDSs	93.60 ± 2.94	95.11 ± 8.68
Remdesivir	79.97 ± 3.55	90.90 ± 4.75

4. Conclusions

The novel nano-formulations of remdesivir based on the hydrophilic, biocompatible bis-MPA PEG6k-OH DLD-polymer present favorable characteristics for application in inhaled aerosols for direct access to the respiratory track. Their structural properties in terms of size and charge are suitable for pulmonary delivery, their hydrophilic nature is compatible with the humid environment of the lungs, their quick remdesivir release and incremental effect on remdesivir solubility assures immediate action on mucus membranes and lung tissue. These qualities, in combination with their non-cytotoxic profile, their ease of preparation and storage stability compared to other type of nanocarriers (like liposomes), make them ideal candidates for the non-invasive administration of remdesivir through the pulmonary route with the advantages of rapid onset of action, improved therapeutic effect and alleviation of systemic toxicity. We hope that this first account on the synthesis, characterization, and toxicity evaluation of the remdesivir-loaded bis-MPA PEG6k-OH nano-formulations will provide insights and serve as a base for further investigations on the utilization of the bis-MPA hyperbranched dendritic scaffolds as carriers of inhaled therapeutics not only against COVID-19, but also against other respiratory diseases.

Author contributions

Conceptualization, E.H.; Methodology, E.H., B.M., C.K. and A. Moschona; Biological assays, B.M.; Investigation, E.H, B.M., M.S., G.L. and M.P.; Resources, E.H, M.P., A. Mitraki and G.L.; Data Curation, E.H. and M.P.; Writing – Original Draft Preparation, E.H, B.M. and M.P.; Writing – Review & Editing, E.H, B.M., M.S., G.L. and M.P.; Supervision, A. Mitraki and M.P.; Project Administration, E.H. and M.P. All authors have read and agreed to the published version of the manuscript.

Declaration of competing interest

The authors declare that they have no known competing financial interests or personal relationships that could have appeared to influence the work reported in this paper.

Data availability

Data will be made available on request.

Acknowledgments

The authors would like to thank Sevasti Papadogiorgaki and Aleka Manousaki, Electron Microscopy Laboratory, Biology Department, University of Crete, for their expert technical assistance with the FESEM observations. Dr. E. Halevas and Dr. B. Mavroidi gratefully acknowledge financial support by Stavros Niarchos Foundation (SNF) through implementation of the program of Industrial Fellowships at NCSR "Demokritos". Dr. E. Halevas also acknowledges the Foundation for Education and European Culture (IPEP) founded by Nicos & Lydia Tricha. Dr. B. Mavroidi also acknowledges the financial support by the State Scholarships Foundation (IKY) through the implementation of the program "Reinforcement of Postdoctoral Researchers−2nd Cycle"(MIS-5033021) (European Social Fund (ESF)−Operational Programme "Human Resources Development, Education and Lifelong Learning".

Appendix A. Supplementary data

Supplementary data to this article can be found online at https://doi.org/10.1016/j.jddst.2022.103625.

Abbreviation list

Bis-MPA	Bis(hydroxymethyl)propionic acid
DLD	Dendritic-Linear-Dendritic
DLS	Dynamic light scattering
EBOV	Ebola virus
EHDSs	Empty HDSs
FESEM	Field emission scanning electron microscopy
FT-IR	Fourier-transform infrared
HDSs	Hyperbranched dendritic scaffolds
MARV	Marburg virus
MERS-CoV	Middle East Respiratory Syndrome-Coronavirus
NiV	Nipah Virus
O/W	Oil-in-water
PBS	Phosphate buffered saline
PEG	Polyethylene glycol
Rem	Remdesivir
RHDSs	Remdesivir-loaded HDSs
RSV	Respiratory Syncytial Virus
SARS-CoV	Severe Acute Respiratory Syndrome-Coronavirus
SBECD	Sulfobutylether B-cyclodextrin

References

[1] M.G. Santoro, E. Carafoli, Remdesivir: from Ebola to COVID-19, Biochem. Biophys. Res. Commun. 538 (2021) 145–150, https://doi.org/10.7573/dic.2020-4-14.
[2] R.T. Eastman, J.S. Roth, K.R. Brimacombe, A. Simeonov, M. Shen, S. Patnaik, M. D. Hall, Remdesivir: a Review of its discovery and development leading to emergency use authorization for treatment of COVID-19, ACS Cent. Sci. 6 (2020) 672–683, https://doi.org/10.1021/acscentsci.0c00489.
[3] C. Scavone, A. Mascolo, C. Rafaniello, L. Sportiello, U. Trama, A. Zoccoli, F. F. Bernardi, G. Racagni, L. Berrino, G. Castaldo, E. Coscioni, F. Rossi, A. Capuano, Therapeutic strategies to fight COVID-19: which is the status artis? Br. J. Pharmacol. (2021) https://doi.org/10.1111/bph.15452 https://doi.org/10.1111/bph.15452.
[4] Summary on compassionate use. Remdesivir. European medicines agency EMA/178637/2020—rev.2, 03 April 2020, https://www.ema.europa.eu/en/documents/other/summary-compassionate-use-remdesivir-gilead_en.pdf. (Accessed 20 November 2021).
[5] D. Sun, Remdesivir for treatment of COVID-19: combination of pulmonary and IV administration may offer additional benefit, AAPS J. 22 (2020) 77, https://doi.org/10.1208/s12248-020-00459-8.
[6] A. Rezagholizadeh, S. Khiali, P. Sarbakhsh, T. Entezari-Maleki, Remdesivir for treatment of COVID-19; an updated systematic review and meta-analysis, Eur. J. Pharmacol. 897 (2021), 173926, https://doi.org/10.1016/j.ejphar.2021.173926.
[7] W.-H. Lee, C.-Y. Loo, D. Traini, P.M. Young, Nano- and micro-based inhaled drug delivery systems for targeting alveolar macrophages, Expet Opin. Drug Deliv. 12 (2015) 1009–1026, https://doi.org/10.1517/17425247.2015.1039509.
[8] A. Zafar, Development of oral lipid based nano-formulation of Dapagliflozin: optimization, *in vitro* characterization and *ex vivo* intestinal permeation study, J. Oleo Sci. 69 (2020) 1389–1401, https://doi.org/10.5650/jos.ess20162.
[9] A. Zafar, N.K. Alruwaili, S.S. Imam, O.A. Alsaidan, K.S. Alharbi, S.I. Alzarea, M. Yasir, M. Afzal, S. Alshehri, A.S. Alanazi, Bioactive luteolin entrapped chitosan-PLGA nanoparticles: formulation optimization to in-vivo preclinical evaluation, J. Cluster Sci. (2022), https://doi.org/10.1007/s10876-022-02232-7.
[10] A. Zafar, N. Khan, N.K. Alruwaili, S.N.A. Bukhari, B. Alsuwayt, M. Afzal, S. Akhter, M. Yasir, M. Elmowafy, K. Shalaby, A. Ali, Improvement of ocular efficacy of levofloxacin by bioadhesive chitosan coated PLGA nanoparticles: box-behnken design, in-vitro characterization, antibacterial evaluation and scintigraphy study, Iran, J. Pharm. Res. 19 (2020) 292–311, https://doi.org/10.22037/ijpr.2019.15318.13016.
[11] N. Khan, A. Zafar, K. Khanna, A. Bhatnagar, F.J. Ahmad, A. Ali, Chitosan coated PLGA nanoparticles amplify the ocular hypotensive effect of forskolin: statistical design, characterization and in vivo studies, Int. J. Biol. Macromol. 116 (2018) 648–663, https://doi.org/10.1016/j.ijbiomac.2018.04.122.

[12] A. Zafar, M. Yasir, N.K. Alruwaili, S.S. Imam, O.A. Alsaidan, S. Alshehri, M. M. Ghoneim, A. Alquraini, A. Rawaf, M.J. Ansari, U.V.S. Sara, Formulation of self-nanoemulsifying drug delivery system of Cephalexin: physiochemical characterization and antibacterial evaluation, Polymers 14 (2022) 1055, https://doi.org/10.3390/polym14051055.

[13] W.-H. Lee, C.-Y. Loo, D. Traini, P.M. Young, Inhalation of nanoparticle-based drug for lung cancer treatment: advantages and challenges, Asian J. Pharm. Sci. 10 (2015) 481–489, https://doi.org/10.1016/j.ajps.2015.08.009.

[14] D. Yang, Application of nanotechnology in the COVID-19 pandemic, Int. J. Nanomed. 16 (2021) 623–649, https://doi.org/10.2147/IJN.S296383.

[15] A. Pandey, A.N. Nikam, S.P. Mutalik, G. Fernandes, A.B. Shreya, B.S. Padya, R. Raychaudhuri, S. Kulkarni, R. Prass, S. Subramanian, A. Korde, S. Mutalik, Architectured therapeutic and diagnostic nanoplatforms for combating SARS-CoV-2: role of inorganic, organic, and radioactive materials, ACS Biomater. Sci. Eng. 7 (2021) 31–54, https://doi.org/10.1021/acsbiomaterials.0c01243.

[16] T. Lammers, A.M. Sofias, R. van der Meel, R. Schiffelers, G. Storm, F. Tacke, S. Koschmieder, T.H. Brümmendorf, F. Kiessling, J.M. Metselaar, Dexamethasone nanomedicines for COVID-19, Nat. Nanotechnol. 15 (2020) 622–624, https://doi.org/10.1038/s41565-020-0752-z.

[17] M. Taher, S.S. Shaari, D. Susanti, Potential nanospray inhalation of remdesivir and hydroxychloroquine using poly (lactic-co-glycolic) acid as fast delivery for Covid-19 treatment, J. Pharm. (Lahore) 1 (2021) 34–44, https://doi.org/10.31436/jop.v1i1.50.

[18] R. Vartak, S.M. Patil, A. Saraswat, M. Patki, N.K. Kunda, K. Patel, Aerosolized nanoliposomal carrier of remdesivir: an effective alternative for COVID-19 treatment in vitro, Nanomedicine (Lond). 16 (2021) 1187–1202, https://doi.org/10.2217/nnm-2020-0475.

[19] M. Ali, Pulmonary drug delivery, in: V.S. Kulkarni (Ed.), Personal Care & Cosmetic Technology, Handbook of Non-invasive Drug Delivery Systems, William Andrew Publishing, Norwich, United States, 2010, pp. 209–246, https://doi.org/10.1016/B978-0-8155-2025-2.10009-5. ISBN 9780815520252,.

[20] https://www.gilead.com/news-and-press/company-statements/gilead-sciences-statement-on-the-initiation-of-clinical-testing-of-an-inhaled-solution-of-remdesivir-for-potential-outpatient-treatment-of-covid19. (Accessed 20 November 2021).

[21] E. Halevas, B. Mavroidi, C. Kokotidou, A. Mitraki, M. Pelecanou, M. Sagnou, Advanced bis-MPA hyperbranched dendritic nanocarriers of artemisinin with anticancer potential, J. Nano Res. 23 (2021) 135, https://doi.org/10.1007/s11051-021-05250-0.

[22] E. Halevas, C. Kokotidou, E. Zaimai, A. Moschona, E. Lialiaris, A. Mitraki, T. Lialiaris, A. Pantazaki, Evaluation of the hemocompatibility and anticancer potential of poly(ε-Caprolactone) and poly(3-Hydroxybutyrate) microcarriers with encapsulated chrysin, Pharmaceutics 13 (2021) 109, https://doi.org/10.3390/pharmaceutics13010109.

[23] O.C.J. Andrén, M.V. Walter, T. Yang, A. Hult, M. Malkoch, Multifunctional poly (ethylene glycol): synthesis, characterization, and potential applications of dendritic–linear–dendritic block copolymer hybrids, Macromolecules 46 (2013) 3726–3736, https://doi.org/10.1021/ma4003984.

[24] E.R. Gillies, J.M.J. Fréchet, Dendrimers and dendritic polymers in drug delivery, Drug Discov. Today 10 (2005) 35–43, https://doi.org/10.1016/S1359-6446(04)03276-3.

[25] Y. Hed, Y. Zhang, O.C.J. Andren, X. Zeng, A.M. Nystrom, M.J. Malkoch, Side-by-side comparison of dendritic-linear hybrids and their hyperbranched analogs as micellar carriers of chemotherapeutics, Polym. Sci., Part A: Polym. Chem. 51 (2013) 3992–3996, https://doi.org/10.1002/pola.26825.

[26] S. Garcia-Gallego, M. Malkoch, Dendritic Polyester Scaffolds: functional and biocompatible precision polymers for drug delivery application. Polymeric drug delivery techniques. Translating polymer Science for drug delivery, Aldrich Mater. Sci., pp. 47-50.

[27] Z. Wu, X. Zeng, Y. Zhang, N. Feliu, P. Lundberg, B. Fadeel, M. Malkoch, A. M. Nyström, Linear-dendritic polymeric amphiphiles as carriers of doxorubicin—*In vitro* evaluation of biocompatibility and drug delivery, J. Polym. Sci., Part A: Polym. Chem. 50 (2012) 217–226, https://doi.org/10.1002/pola.25008.

[28] P. Lundberg, M.V. Walter, M.I. Montañez, D. Hult, A. Hult, A. Nyström, M. Malkoch, Linear dendritic polymeric amphiphiles with intrinsic biocompatibility: synthesis and characterization to fabrication of micelles and honeycomb membranes, Polym. Chem. 2 (2011) 394–402, https://doi.org/10.1039/C0PY00258E.

[29] Z. Datki, A. Juhász, M. Gálfi, K. Soós, R. Papp, D. Zádori, B. Penke, Method for measuring neurotoxicity of aggregating polypeptides with the MTT assay on differentiated neuroblastoma cells, Brain Res. Bull. 62 (2003) 223–229, https://doi.org/10.1016/j.brainresbull.2003.09.011.

[30] B.P. McSharry, C.J. Jones, J.W. Skinner, D. Kipling, G.W.G. Wilkinson, Human telomerase reverse transcriptase-immortalized MRC-5 and HCA2 human fibroblasts are fully permissive for human cytomegalovirus, J. Gen. Virol. 82 (2001) 855–863, https://doi.org/10.1099/0022-1317-82-4-855.

[31] H.D. Nguea, A. de Reydellet, A. Le Faou, M. Zaiou, B. Rihn, Macrophage culture as a suitable paradigm for evaluation of synthetic vitreous fibers, Crit. Rev. Toxicol. 38 (2008) 675–695, https://doi.org/10.1080/10408440802194915.

[32] J.S. Suk, Q. Xu, N. Kim, J. Hanes, L.M. Ensign, PEGylation as a strategy for improving nanoparticle-based drug and gene delivery, Adv. Drug Deliv. Rev. 99 (2016) 28–51, https://doi.org/10.1016/j.addr.2015.09.012.

[33] M. Irfan, M. Seiler, Encapsulation using hyperbranched polymers: from research and technologies to emerging applications, Ind. Eng. Chem. Res. 49 (2010) 1169–1196, https://doi.org/10.1021/ie900216r.

[34] I. Tanis, K. Karatasos, Association of a weakly acidic anti-inflammatory drug (Ibuprofen) with a poly(amidoamine) dendrimer as studied by molecular dynamics simulations, J. Phys. Chem. B 113 (2009) 10984–10993, https://doi.org/10.1021/jp9039176.

[35] PubChem compound summary – Remdesivir. https://pubchem.ncbi.nlm.nih.gov/compound/Remdesivir#section=Chemical-and-Physical-Properties. (Accessed 20 November 2021).

[36] J. Jang, J.H. Oh, In situ FT-IR spectroscopic investigation on the microstructure of hyperbranched aliphatic polyesters, Polymer 40 (1999) 5985–5992, https://doi.org/10.1016/S0032-3861(98)00824-6.

[37] A.R. Polu, R. Kumar, Impedance spectroscopy and FTIR studies of PEG-based polymer electrolytes, J. Chem. 8 (2011) 347–353, https://doi.org/10.1155/2011/628790.

[38] T.D. Nguyen, S. Chang, B. Condon, M. Uchimiya, C. Fortier, Development of an environmentally friendly halogen-free phosphorous-nitrogen bond flame retardant for cotton fabrics, Polym, Adv. Met. Technol. 23 (2012) 1555–1563, https://doi.org/10.1002/pat.3029.

[39] H. Wang, Y. Cai, Z. Jiang, S. Guo, P. Zhu, Synthesis of a phosphoramidate flame retardant and its flame retardancy on cotton fabrics, E-Polymers 20 (2020) 550–560, https://doi.org/10.1515/epoly-2020-0059.

[40] Z. Shariatinia, M. Sohrabi, M. Yousefi, T. Koval, M. Dusek, X-Ray crystallography of a new phosphoramidate; Synthesis and spectroscopic investigation, Heteroat. Chem. 23 (2012) 478–485, https://doi.org/10.1107/S0108768110018550.

[41] C. He, Y. Hu, L. Yin, C. Tang, C. Yin, Effects of particle size and surface charge on cellular uptake and biodistribution of polymeric nanoparticles, Biomaterials 31 (2010) 3657–3666, https://doi.org/10.1016/j.biomaterials.2010.01.065.

[42] X. Zeng, Y. Zhang, Z. Wu, P. Lundberg, M. Malkoch, A.M. Nyström, Hyperbranched copolymer micelles as delivery vehicles of doxorubicin in breast cancer cells, J. Polym. Sci. Polym. Chem. (2012) 280–288, https://doi.org/10.1002/pola.25027.

[43] S.M.A. Sadat, S.T. Jahan, A. Haddadi, Effects of size and surface charge of polymeric nanoparticles on in vitro and in vivo applications, J. Biomater. Nanobiotechnol. 7 (2016) 91–108, https://doi.org/10.4236/jbnb.2016.72011.

[44] R. Zein, W. Sharrouf, K. Selting, Physical properties of nanoparticles that result in improved cancer targeting, JAMA Oncol. 2020 (2020), https://doi.org/10.1155/2020/5194780. Article ID 5194780.

[45] S. Suttiruengwong, J. Rolker, I. Smirnova, W. Arlt, M. Seiler, L. Lüderitz, Y. Pérez de Diego, P.J. Jansens, Hyperbranched polymers as drug carriers: microencapsulation and release kinetics, Pharmaceut. Dev. Technol. 11 (2006) 55–70, https://doi.org/10.1080/10837450500463919.

[46] C. Kojima, K. Kono, K. Maruyama, T. Takagishi, Synthesis of polyamidoamine dendrimers having poly(ethylene glycol) grafts and their ability to encapsulate anticancer drugs, Bioconjugate Chem. 11 (2000) 910–917, https://doi.org/10.1021/bc0000583.

[47] P. Kolhe, E. Misra, R.M. Kannan, S. Kannan, M. Lieh-Lai, Drug complexation, in vitro release and cellular entry of dendrimers and hyperbranched polymers, Int. J. Pharm. 259 (2003) 143–160, https://doi.org/10.1016/S0378-5173(03)00225-4.

[48] B. Magenheim, M.Y. Levy, S. Benita, A new in vitro technique for the evaluation of drug release profile from colloidal carriers - ultrafiltration technique at low pressure, Int. J. Pharm. 94 (2013) 115–123, https://doi.org/10.1016/0378-5173(93)90015-8.

[49] R. Singh, J.W. Lillard Jr., Nanoparticle-based targeted drug delivery, Exp. Mol. Pathol. 86 (2009) 215–223, https://doi.org/10.1016/j.yexmp.2008.12.004.

[50] L. Szente, I. Puskás, T. Sohajda, E. Varga, P. Vass, Z.K. Nagy, A. Farkas, B. Várnai, S. Béni, E. Hazai, Sulfobutylether-beta-cyclodextrin-enabled antiviral remdesivir: characterization of electrospun- and lyophilized formulations, Carbohydr. Polym. 264 (2021), 118011, https://doi.org/10.1016/j.carbpol.2021.118011.

[51] R. Gouda, H. Baishya, Z. Qing, Application of mathematical models in drug release kinetics of Carbidopa and Levodopa ER tablets, J. Develop. Drugs. 6 (2017) 2, https://doi.org/10.4172/2329-6631.1000171.

[52] G. Soni, K.S. Yadav, High encapsulation efficiency of poloxamer-based injectable thermoresponsive hydrogels of etoposide, Pharmaceut. Dev. Technol. 19 (2014) 651–661, https://doi.org/10.3109/10837450.2013.819014.

[53] K. Jiyauddin, Y.K. Sung, A.D. Samer, M. Kaleemullah, S. Rasha, S. Budiasih, A. Jawad, M.R. Rasny, O.E. Gamal, A.H. Junainah, Y. Eddy, A. Fadli, W.J. Chan, Comparative study on the effect of hydrophilic and hydrophobic polymers on the dissolution rate of a poorly water soluble drug, IJPAR 3 (2014) 291–300.

[54] D. Wojcik-Pastuszka, J. Krzak, B. Macikowski, R. Berkowski, B. Osiński, W. Musiał, Evaluation of the release kinetics of a pharmacologically active substance from model intra-articular implants replacing the cruciate ligaments of the knee, Materials 12 (2019) 1202, https://doi.org/10.3390/ma12081202.

[55] Mathematical models of drug release, in: M.L. Bruschi (Ed.), Strategies to Modify the Drug Release from Pharmaceutical Systems, Woodhead Publishing, 2015, pp. 63–86, https://doi.org/10.1016/B978-0-08-100092-2.00005-9.

[56] K. Parang, N.S. El-Sayed, A.J. Kazeminy, R.K. Tiwari, Comparative antiviral activity of remdesivir and anti-HIV nucleoside analogs against human coronavirus 229E (HCoV-229E), Molecules 25 (2020) 2343, https://doi.org/10.3390/molecules25102343.

[57] S. Tao, K. Zandi, L. Bassit, Y.T. Ong, K. Verma, P. Liu, J.A. Downs-Bowen, T. McBrayer, J.C. LeCher, J.J. Kohler, P.R. Tedbury, B. Kim, F. Amblard, S. G. Sarafianos, R.F. Schinazi, Comparison of anti-SARS-CoV-2 activity and intracellular metabolism of remdesivir and its parent nucleoside, CRPHAR 2 (2021), 100045, https://doi.org/10.1016/j.crphar.2021.100045.